Microporous and Mesoporous Materials 220 (2016) 253–257

Contents lists available at ScienceDirect

Microporous and Mesoporous Materials

journal homepage: www.elsevier.com/locate/micromeso

Short communication

Molecular transport properties of ZIF-8 thin films in aqueous environments: The critical role of intergrain mesoporosity as diffusional pathway

Jimena S. Tuninetti [a], Matías Rafti [a], Annette Andrieu-Brunsen [b], Omar Azzaroni [a, *]

[a] Instituto de Investigaciones Fisicoquímicas Teóricas y Aplicadas (INIFTA), Departamento de Química, Facultad de Ciencias Exactas, Universidad Nacional de La Plata, CONICET, CC 16 Su. 4, 1900 La Plata, Argentina
[b] Department of Chemistry, LOEWE "Soft Control", Technische Universität Darmstadt, Alarich-Weiss-Str. 4, 64287 Darmstadt, Germany

ARTICLE INFO

Article history:
Received 8 July 2015
Received in revised form
13 August 2015
Accepted 28 August 2015
Available online 11 September 2015

Keywords:
Metal-organic frameworks
ZIF-8
Thin films
Molecular transport

ABSTRACT

We report here the first use of electrochemical tools to quantify molecular transport from aqueous solutions into ZIF-8 MOF thin films. Our experimental findings reveal that molecular transport through ZIF-8 films in aqueous environments is purely dominated by solvent-filled intergrain mesoporosity and exhibits two well-defined transport regimes.

1. Introduction

Metal-organic frameworks (MOFs) represent one of the most exciting research areas in modern materials science [1–7]. In recent years research on MOFs has extended from bulk synthesis, to thin film engineering, to the microscopic study of molecular dynamics and structure (i.e., the molecular level understanding of these systems) [8,9]. Particularly, the generation and use of thin films of MOFs has attracted significant attention due to their integration in chemical sensors, catalysts, and also optical devices [10–13]. These materials represent a versatile class of crystalline hybrid inorganic–organic solids exhibiting wide structural diversity with pore sizes ranging from a few angstroms to several nanometres and specific surface areas exceeding that of traditional adsorbents. These features have made MOFs the focal point of many studies focussed on their adsorption properties. However, their performance for practical capture, storage and release applications critically depends on the diffusion and interaction of probe molecules in the MOF environment. For instance, in most applications of MOFs it is crucial to rely on quantitative information on diffusion of guest molecules within the host framework. While there has been considerable progress in recent years with regard to the understanding of molecular transport through MOFs in gas phase systems [14], very little is known about diffusion of molecules through solvent-filled MOFs [15]. This lack of information is even more striking in the context of molecular transport through intergrain voids in MOF thin films with hierarchical porosity. This aspect is particularly relevant in view of the potential applications of MOFs in liquid-phase separation [16], biocompatible materials for drug delivery [17,18], and chemical sensing [19]. For the use of MOFs as catalysts [20], hierarchical intercrystalline porosity is one of the most important aspects since it determines to a large extent the accessibility of reactive sites and the speed at which reactants can reach these sites within the porous structure [21]. In this regard, Sanchez, Serre, and co-workers [22–24], developed an interesting strategy to fabricate MOF thin films by assembly of colloidal MOF particles onto solid surfaces. A most appealing aspect of this strategy is the control over intergrain mesoporosity that, in turn, enables easier diffusion of analytes into the film. Formation of MOF thin films displaying hierarchical porosity [25,26] can also be attained by the method of seeding and secondary growth. This strategy relies on the impregnation of the substrate surface with an

* Corresponding author. Tel.: +54 221 425 7430; fax: +54 221 425 4642.
E-mail address: azzaroni@inifta.unlp.edu.ar (O. Azzaroni).
URL: http://softmatter.quimica.unlp.edu.ar

http://dx.doi.org/10.1016/j.micromeso.2015.08.035
1387-1811/

aged precursor solution containing the MOF seeds and permits separate control of MOF nucleation and growth steps. As a result, sequential impregnation steps enable the layer-by-layer formation of thick MOF films displaying mesoporous intercrystalline voids [27].

When considering solvent-filled MOFs in thin film formats, the elucidation of molecular transport mechanisms through mesoporous spaces and the concomitant estimation of diffusivities are increasingly important in the up-and-coming electrochemical applications of these materials [28]. It has long been considered that molecular transport through MOFs can be described as a simple Fickian diffusion. However, this vision changed after Grzybowski and co-workers demonstrated that considering a pure diffusion approach is a gross oversimplification and suggested that surface-governed processes are operative [29]. Taking into account these notions and being aware of the critical role of intergrain porosity in defining the molecular transport characteristics of MOF thin films we took this new paradigm one step further by exploring the use of electrochemical techniques to unravel the mechanisms governing the diffusion of molecules through intergranular voids in solvent-filled, hierarchically porous MOFs at the solid–liquid interface. The diversity of methodological approaches to quantify the molecular transport in MOFs is of varied complexity and applicability.

Among the techniques used quasi-elastic neutron scattering (QENS) [30], pulsed field gradient nuclear magnetic resonance (PFG NMR) [31], fluorescence correlation spectroscopy (FCS) [29], and quartz crystal microbalance (QCM) [32], can be mentioned.

Within the context of matching science to application, the use of electrochemical tools offers the possibility of exploring the inner environment of the porous material, studying transient transport processes, and estimating diffusion coefficients through simple experiments using readily available equipment [33,34].

The aims of the research presented herein are three-fold: to introduce a simple method to study the diffusion of probe molecules through solvent-filled MOF thin films, to elucidate the mechanisms that govern molecular transport through intergrain mesoporosity in MOFs, and to estimate the diffusivity of probe molecules permeating through solvent-filled MOF layers. To meet these goals, we exploited the versatility of electrochemistry to detect the diffusion of redox-active tracers (excluded from micropores) permeating through the MOF film and reaching a conductive substrate.

2. Experimental

2.1. Synthesis of ZIF-8 thin films

ZIF-8 films were synthesized over chemically modified ITO coated glass (Delta Technologies) using methanolic solutions of precursors according to previously published procedure [35,36]. Briefly, it consists of the following steps: i) clean ITO coated glass substrates were treated with APTES/Toluene solution at 110 °C for 2 h (0.2 mM APTES in 10 mL Toluene), then rinsed, and heated at 100 °C for 10 min, ii) modified ITO substrates were immersed in a fresh mixture of $Zn(NO_3)_2.6H_2O$ (25 mM) + 2-methyl-Imidazole (50 mM) stock solutions for 40 min at room temperature, iii) substrates were then rinsed with fresh methanol and dried with N_2 prior to the next cycle. Films grown under these conditions were reported to increase ≈65 nm per cycle. APTES forms a self assembled monolayer that acts as an initiator of the enhanced heterogeneous nucleation process (via Zn^{2+} ion coordination). The samples were dried at moderate temperatures (50 °C) before use. Characterization of films obtained confirming the presence of ZIF-8 was performed via Scanning Electron Microscopy, ATR-FTIR, water contact angle, X-ray diffraction and Nitrogen adsorption isotherms, and is given in Supplementary Material. Fig. 1 shows a comparison of the diffractogram obtained for the different materials synthesized.

2.2. Water uptake via quartz crystal microbalance (QCM)

Experiments for determining water uptake of ZIF-8 films were carried using a flow cell Quartz Crystal Microbalance (QCM200 Stanford Research Systems) setup. For each experiment, the MOF films were grown in situ following the same procedure as described above, in such way that the weight of ZIF-8 per unit area was a known parameter, and thus water uptake could be normalized. The flow cell was equilibrated with dry N_2 at a flow rate of 30 mL/min and then treated with water saturated N_2. Water saturated N_2 flow was achieved by directing dry N_2 through a bubbler at a flow rate of 30 mL/min. The bubbler was filled with deionized water and N_2 bubbles were forced to flow through. Water saturated N_2 flow was established, and weight increment was followed on the QCM until a plateau was reached (i.e., saturation of the film adsorption capacity), see Supplementary Material for more details on the setup.

2.3. Cyclic voltammetry experiments

Cyclic voltammetry experiments were carried out using a potentiostat Reference 600 from Gamry, with a three-electrode setup. Ag/AgCl and Pt wire were used as reference electrode and counter electrodes, respectively. In all the electrochemical experiments 1 mM $Fe(CN)_6^{3-}/Fe(CN)_6^{4-}$ + 100 mM KCl solutions were used.

3. Results and discussion

Zeolitic imidazolate framework (ZIF)-8 films were successfully synthesized over indium tin oxide (ITO)-coated supports at room temperature from stoichiometric methanolic precursor solutions using sequential one-pot procedure (see Supplementary Material for XRD characterization). The intercrystalline molecular transport through the MOF thin films was electrochemically probed using electroactive $Fe(CN)_6^{3-}$ species diffusing across films of

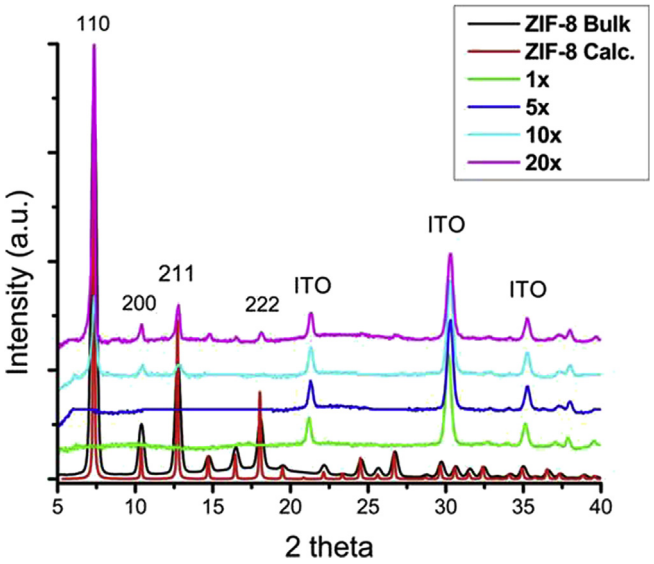

Fig. 1. XRD corresponding to the various ZIF-8 films synthesized over ITO substrates. Both calculated and experimentally obtained ZIF-8 bulk material diffractograms are also displayed for comparison.

different thickness deposited on conductive ITO substrates. Given the molecular dimensions of the redox-active permeant molecule (6 Å × 6 Å × 6 Å) [37], $Fe(CN)_6^{3-}$ species can be employed to effectively assess intergrain diffusion provided that they are too large to pass through intragrain MOF pores, i.e.: micropores, with nominal crystallographic aperture size of 3.4 Å. Hence, in our experiments size exclusion effects prevent micropores from being accessed by $Fe(CN)_6^{3-}$ and consequently electrochemical signals arise from the passage of electroactive tracers through intergrain voids in the MOF thin film. Fig. 2 displays the temporal evolution of cyclic voltammograms of ZIF-8 films supported on ITO in the presence of 1 mM $Fe(CN)_6^{3-}$.

What is the most interesting aspect of this evolution is not the quantitative, but the qualitative transformation of the electrochemical signal as time proceeds. Quantitative changes are expected provided that the permeation of electroactive $Fe(CN)_6^{3-}$ species through the MOF film into the surroundings of the ITO electrode must lead to an increase in the electrochemical signal. However, the qualitative transformation of the cyclic voltammograms indicates changes in the local conditions of the redox probes taking place during the permeation process. The electrochemical response reveals that electron transfer is initially affected by strong resistive effects that influence the peak profile so that the peak is flattened and shifted toward more negative (cathodic peak) or more positive (anodic peak) potentials. The peak separation, ΔE_p, in this case is ~400 mV. The sluggish redox process is likely the result of both the surface effects leading to slow electron transfer and the slow diffusion through the intercrystalline cavities. However, we observed that after 10–20 min the electrochemical response evolved into nearly ideal electron transfer kinetics of the redox probes on the ZIF-8-modified ITO electrodes.

The voltammetric response corresponds to the reversible one-electron reduction of $Fe(CN)_6^{3-}$ and the peak-shaped voltammograms are indicative of an electrochemical reaction limited by diffusional transport of the reactant to the electrode surface.

Real-time tracking of the electrochemical signal clearly indicates that the molecular transport through intergrain mesoporosity cannot be described by a simple Fickian diffusion (Fig. 3). This is an important finding that has strong implications for many electrochemical applications of MOFs; e.g., proton conducting membranes

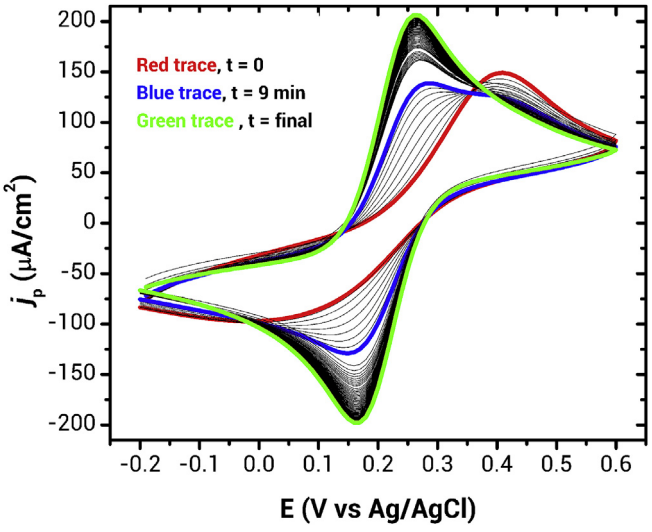

Fig. 2. Temporal evolution of the voltammetric response for a ZIF-8-modified ITO electrode (one MOF deposition cycle) in the presence of 1 mM $Fe(CN)_6^{3-}$ + 100 mM KCl (aqueous solution).

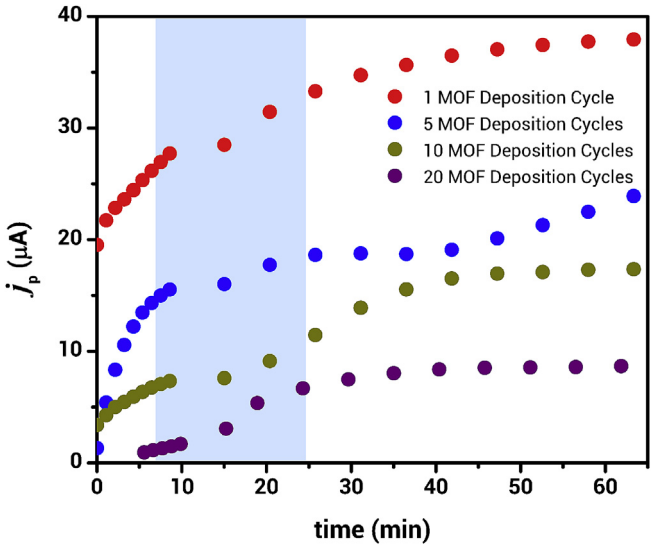

Fig. 3. Time evolution of the voltammetric peak current density (j_p) for different ZIF-8-modified ITO electrodes. Different colours correspond to 1 (red), 5 (blue), 10 (green) and 20 (purple) MOF deposition cycles. (For interpretation of the references to colour in this figure legend, the reader is referred to the web version of this article.)

[38]. We observed that the transport process takes place in two well-defined temporal domains (Fig. 3). First, the redox probes permeate through the MOF thin films under pronounced resistive conditions (see early stages in Fig. 2) reaching a pseudo-plateau. This scenario prevails during the initial 10–20 min irrespective of the thickness of the MOF layer deposited on the ITO electrode. Then, the resistive effects cease and a marked increase in the electrochemical signal occurs.

The above discussed change in response, which is also accompanied with a major improvement in the electrochemical reversibility, can be rationalized as a consequence of the facilitated influx of $Fe(CN)_6^{3-}$ ions, which ultimately causes the electrochemical signal to reach a stable plateau. To understand the presence of resistive effects during the initial steps we need to consider the marked hydrophobicity of ZIF-8 materials. Recent report by Chance et al. [39] demonstrated that hydrophobicity of ZIF-8 precludes the adsorption of water within the MOF micropores and consequently the cage-filling phenomenon is not observed. In the case of the molecular transport through intergrain mesopores the hydrophobic nature of the confined environment prevents the rapid wetting and passage of the electrolyte solution and consequently a progressive filling of the pores is electrochemically detected. Regarding this fact, we should note that similar observations were reported for electrodes functionalized with carbon nanotubes. Poor wetting properties of functionalized carbon nanotubes were found to have deleterious effects on the electron transfer kinetics of $Fe(CN)_6^{3-/4-}$ redox couple [40].

To gain more insight into the dynamics of the process, we studied kinetics of water uptake via quartz crystal microbalance experiments (Fig. 4). Room temperature, water-saturated nitrogen streams were passed over the ZIF-8 films grown in-situ over QCM crystals, and assembled into a flow cell (see Supplementary Material for details). Microgravimetric studies indicated that the amount of water permeating into the film was proportional to the film thickness (445 nm and 610 nm for 5 and 10 sequential growth cycles respectively), as determined via ellipsometric measurements, thus confirming that the uptake process occurs at the MOF film inner environment. This implies that according to Chance and co-workers [39], water molecules are excluded from ZIF-8

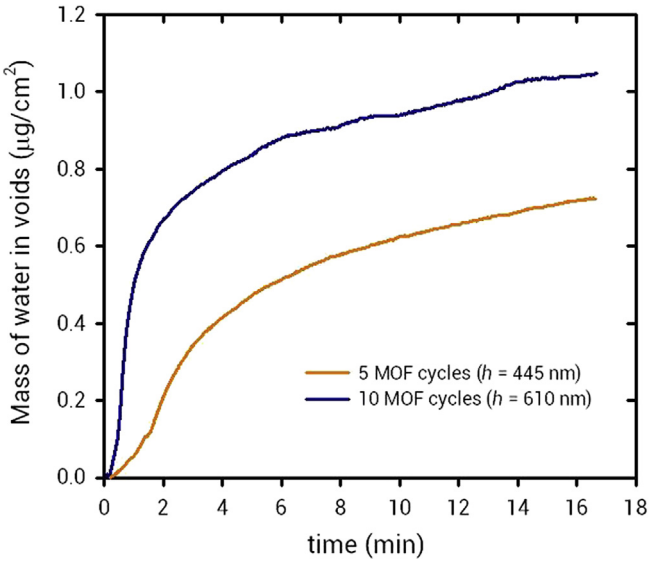

Fig. 4. Quartz crystal microbalance (QCM) water uptake curves for two ZIF-8 films of increasing thickness (445 and 610 nm for 5 and 10 synthesis cycles respectively, as determined via ellipsometry).

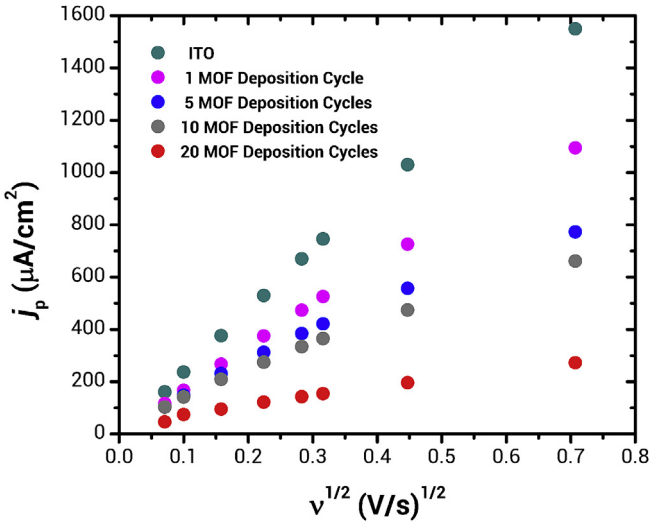

Fig. 5. Plots of voltammetric peak current density (j_p) versus square root of the scan rate ($\nu^{1/2}$) for bare ITO and several ZIF-8-modified ITO electrodes prepared with increasing number of deposition cycles.

micropores; but concomitantly, our QCM experiments indicates that water molecules can access the mesopores. Interestingly, the time needed for water saturation of films with different thickness remains constant at a given flow rate. This would explain why in Fig. 3 we observe two regimes, and the transition between regimes occurs on similar timescales regardless of film thickness. The first stage of probe diffusion is governed by solvent permeation, then in solvent-filled intergrain mesopores the redox probes are electrochemically accessible because they have enough mobility to diffuse through the pores on the timescale of the voltammetric experiment, with peak potentials located at the same value as for $Fe(CN)_6^{3-}$ in solution. In the above discussed scenario, the diffusion coefficient of $Fe(CN)_6^{3-}$ can be readily obtained by measuring the voltammetric peak current density, j_p, as a function of scan rate, ν. For a diffusion-controlled electron transfer, the value of j_p is proportional to the square root of ν:

$$j_p = 0.4463nFC\,(nF/RT)^{1/2}\nu^{1/2}D^{1/2} \quad (1)$$

where D represents the effective diffusion coefficient of $Fe(CN)_6^{3-}$ species, F is Faraday's constant, C is the bulk concentration of $Fe(CN)_6^{3-}$, n is the number of electrons transferred, R is the molar gas constant, and T is temperature. The slope of a plot of j_p vs. $\nu^{1/2}$ yields D.

Fig. 5 shows such j_p vs. $\nu^{1/2}$ plots for ITO electrodes modified with ZIF-8 films of several thicknesses. As expected from eq. (1), a linear dependence j_p vs. $\nu^{1/2}$ is obtained in all cases. Estimated values of D are 3.2×10^{-6}, 1.5×10^{-6}, 1.0×10^{-6} and 0.16×10^{-6} cm^2/s for ZIF-8 films grown through 1, 5, 10 and 20 deposition cycles, respectively. The diffusion coefficient of $Fe(CN)_6^{3-}$ species in the bulk solution was found to be equal to 6.6×10^{-6} cm^2/s. The latter value is in excellent agreement with the accepted literature value, 6.5×10^{-6} cm^2/s in 0.1 M KCl [41]. It is evident that film thickness has an influence on the diffusivity of the redox probes provided that MOF films grown by 20 deposition cycles exhibited a one-order-of-magnitude decrease in diffusivity as compared with films grown by one single deposition cycle (Fig. 6). We infer that the influence of film thickness originates from changes in tortuosity upon increasing the number of deposition cycles. Tortuosity is mainly governed by the pore network topology and plays a significant role in defining how the material structure affects the motion of guest molecules. As is well-known, an increase in tortuosity leads to a decrease in effective electrolyte diffusivity [42].

In our case, the experimental observations suggest that the increasing number of MOF layers integrated into the film increases the tortuosity of the diffusional path around the impenetrable crystals with the concomitant decrease in $Fe(CN)_6^{3-}$ diffusivity. For instance, it has been demonstrated that permeances may be greatly reduced by misoriented grains and intergrain boundaries [43]. Our hypothesis is that upon adding new layers to the MOF film there is an increasing number of micro-heterogeneities in the film volume that ultimately leads to a more tortuous microstructure.

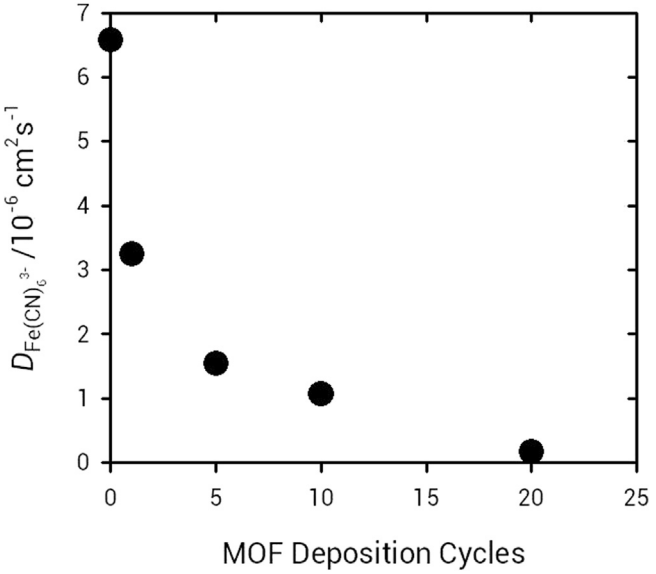

Fig. 6. Representation of the effective diffusion coefficient of $Fe(CN)_6^{3-}$ probes as a function of the number of deposition cycles required to grow the ZIF-8 layer.

4. Conclusions

We reported for the first time the use of electrochemical tools to quantify molecular transport from aqueous solutions into ZIF-8 metal-organic framework thin films. Our experimental findings reveal conclusively that molecular transport through ZIF-8 films in aqueous environments is purely dominated by solvent-filled intergrain mesoporosity. This observation is crucially important to attain a more realistic picture of ZIF-8 thin films in multiple applications. For instance, molecular-level descriptions of aqueous electrochemical processes taking place in ZIF-8 should be more accurate by taking better account of the intergrain diffusion, especially if we consider that water is excluded from micropores. Time-resolved measurements suggest that the hydrophobic nature of ZIF-8 plays a role in retarding the entrance of solvent into the mesopores, but after several minutes the redox tracers are able to diffuse through the solvent-filled pores on the timescale of the electrochemical experiments. This interplay between solvent permeation and probe diffusion is reflected by the existence of two well-defined transport regimes. To the best of our knowledge this is the first observation of such a behaviour in solvent-filled MOFs. Finally, we were able to estimate diffusivity values for the redox traces permeating into the film. We observed that diffusivity values strongly depend on the number of MOF layers deposited on the electrode support, which might suggest an increase in tortuosity with film thickness.

These simple yet crucial experiments should be taken into account when attempting new settings of MOFs in aqueous environments, for example, the design of metal nanoparticle-MOF composites for electrocatalytic purposes or the use of MOFs for drug delivery applications. We believe that these results lead to significant progress in understanding molecular transport in solvent-filled MOFs and will have direct relevance in furthering our control of their transport properties as well as provide new insights into the dynamics of molecular diffusion into nanomaterials displaying hierarchical porosity.

Acknowledgements

J.T gratefully acknowledges CONICET for a postdoctoral fellowship. This work was supported by CONICET (PIP 11220130100370CO), ANPCyT (PICT-2010-2554 and PICT-2013-0905). M.R. and O.A. are CONICET fellows.

Appendix A. Supplementary data

Supplementary data related to this article can be found at http://dx.doi.org/10.1016/j.micromeso.2015.08.035.

References

[1] M. Li, D. Li, M. O'Keeffe, O.M. Yaghi, Chem. Rev. 114 (2014) 1343.
[2] H. Furukawa, K.E. Cordova, M. O'Keeffe, O.M. Yaghi, Science 341 (2013) 974.
[3] X. Kong, H. Deng, F. Yan, J. Kim, J.A. Swisher, B. Smit, O.M. Yaghi, J.A. Reimer, Science 341 (2013) 882.
[4] H. Deng, S. Grunder, K.E. Cordova, C. Valente, H. Furukawa, M. Hmadeh, F. Gandara, A.C. Whalley, Z. Liu, S. Asahina, H. Kazumori, M. O'Keeffe, O. Terasaki, J.F. Stoddart, O.M. Yaghi, Science 336 (2012) 1018.
[5] C. Serre, Angew. Chem. Int. Ed. 51 (2012) 6048.
[6] M.C. So, S. Jin, H.J. Son, G.P. Wiederrecht, O.K. Farha, J.T. Hupp, J. Am. Chem. Soc. 135 (2013) 15698.
[7] R.A. Fischer, C. Wöll, Angew. Chem. Int. Ed. 47 (2008) 8164.
[8] J. Čejka, Angew. Chem. Int. Ed. 51 (2012) 4782.
[9] Y.S. Li, H. Bux, A. Feldhoff, G.N. Li, W.S. Yang, J. Caro, Adv. Mater. 22 (2010) 3322.
[10] O. Shekhah, H. Wang, D. Zacher, R.A. Fischer, C. Wöll, Angew. Chem. Int. Ed. 48 (2009) 5038.
[11] O. Shekhah, J. Liu, R.A. Fischer, C. Wöll, Chem. Soc. Rev. 40 (2011) 1081.
[12] D. Zacher, O. Shekhah, C. Wöll, R.A. Fischer, Chem. Soc. Rev. 38 (2009) 1418.
[13] A. Schoedel, C. Scherb, T. Bein, Angew. Chem. Int. Ed. 49 (2010) 7225.
[14] J.-R. Li, R.J. Kuppler, H.-C. Zhou, Chem. Soc. Rev. 38 (2009) 1477.
[15] C. Wang, W. Lin, J. Am. Chem. Soc. 133 (2011) 4232.
[16] L. Alaerts, M. Maes, L. Giebeler, P.A. Jacobs, J.A. Martens, J.F.M. Denayer, C.E.A. Kirschhock, D.E. De Vos, J. Am. Chem. Soc. 130 (2008) 14170.
[17] P. Horcajada, T. Chalati, C. Serre, B. Gillet, C. Sebrie, T. Baati, J.F. Eubank, D. Heurtaux, P. Clayette, C. Kreuz, J.-S. Chang, Y.K. Hwang, V. Marsaud, P.-N. Bories, L. Cynober, S. Gil, G. Férey, P. Couvreur, R. Gref, Nat. Mater. 9 (2010) 172.
[18] J.G. Yañuk, M.L. Alomar, M.M. Gonzalez, F. Simon, R. Erra-Balsells, M. Rafti, F.M. Cabrerizo, Phys. Chem. Chem. Phys. 17 (2015) 12462.
[19] B. Chen, L. Wang, Y. Xiao, F.R. Fronczek, M. Xue, Y. Cui, G. Qian, Angew. Chem. Int. Ed. 48 (2009) 500.
[20] D. Farrusseng, S. Aguado, C. Pinel, Angew. Chem. Int. Ed. 48 (2009) 7502.
[21] F.X.L. Xamena, J. Gascon, Metal Organic Frameworks as Heterogeneous Catalysts, Royal Society of Chemistry, 2013.
[22] A. Demessence, C. Boissière, D. Grosso, P. Horcajada, C. Serre, G. Férey, G.J.A.A. Soler-Illia, C. Sanchez, J. Mater. Chem. 20 (2010) 7676.
[23] P. Horcajada, C. Serre, D. Grosso, C. Boissière, S. Perruchas, C. Sanchez, G. Férey, Adv. Mater. 21 (2009) 1931.
[24] A. Demessence, P. Horcajada, C. Serre, C. Boissière, D. Grosso, C. Sanchez, G. Férey, Chem. Commun. 46 (2009) 7149.
[25] L.D. O'Neill, H. Zhang, D. Bradshaw, J. Mater. Chem. 20 (2010) 5720.
[26] D. Bradshaw, A. Garai, J. Huo, Chem. Soc. Rev. 41 (2012) 2344.
[27] S. Furukawa, J. Reboul, S. Diring, K. Sumida, S. Kitagawa, Chem. Soc. Rev. 43 (2014) 5700.
[28] A. Morozan, F. Jaouen, Energy Environ. Sci. 5 (2012) 9269.
[29] S. Han, T.M. Hermans, P.E. Fuller, Y. Wei, B.A. Grzybowski, Angew. Chem. Int. Ed. 51 (2012) 2662.
[30] F. Salles, H. Jobic, T. Devic, P.L. Llewellyn, C. Serre, G. Férey, G. Maurin, ACS Nano 4 (2010) 143.
[31] F. Stallmach, S. Gröger, V. Künzel, J. Kärger, O.M. Yaghi, M. Hesse, U. Müller, Angew. Chem. Int. Ed. 45 (2006) 2123.
[32] L. Heinke, C. Woll, Phys. Chem. Chem. Phys. 15 (2013) 9295.
[33] I. Rubinstein, Physical Electrochemistry: Principles, Methods, and Applications, Marcel Dekker, Inc., New York, 1995.
[34] A.J. Bard, L.R. Faulkner, Electrochemical Methods: Fundamentals and Applications, Wiley, New York, 2000.
[35] C. Hou, Q. Xu, J. Peng, Z. Ji, X. Hu, ChemPhysChem 14 (2013) 140.
[36] K. Kida, K. Fujita, T. Shimada, S. Tanaka, Y. Miyake, Dalt. Trans. 42 (2013) 11128.
[37] A.J. Bard, M. Stratmann, I. Rubinstein, M. Fujihira, J.F. Rusling, Encyclopedia of Electrochemistry: Modified Electrodes, vol. 10, Wiley-VCH, Weinheim, 2007.
[38] W.J. Phang, W.R. Lee, K. Yoo, D.W. Ryu, B. Kim, C.S. Hong, Angew. Chem. Int. Ed. 53 (2014) 8383.
[39] K. Zhang, R.P. Lively, M.E. Dose, A.J. Brown, C. Zhang, J. Chung, S. Nair, W.J. Koros, R.R. Chance, Chem. Commun. 49 (2013) 3245.
[40] P. Papakonstantinou, R. Kern, L. Robinson, H. Murphy, J. Irvine, E. McAdams, J. McLaughlin, T. McNally, Fullerenes Nanotub. Carbon Nanostruct. 13 (2005) 91.
[41] M.R. Newton, K.A. Morey, Y. Zhang, R.J. Snow, M. Diwekar, J. Shi, H.S. White, Nano Lett. 4 (2004) 875.
[42] M. Ebner, D.W. Chung, R.E. García, V. Wood, Adv. Energy Mater. 4 (2014) 1.
[43] R. Ranjan, M. Tsapatsis, Chem. Mater. 21 (2009) 4920.